

High-order multiphoton laser-assisted elastic electron scattering by Xe in a femtosecond near-infrared intense laser field: Plateau in energy spectra of scattered electrons

Kakuta Ishida, Yuya Morimoto,* Reika Kanya, and Kaoru Yamanouchi†

Department of Chemistry, School of Science, The University of Tokyo, 7-3-1 Hongo, Bunkyo-ku, Tokyo 113-0033, Japan

(Received 26 December 2016; published 21 February 2017)

Multiphoton free-free transitions were observed in laser-assisted elastic electron scattering (LAES) by Xe atoms in a femtosecond near-infrared intense laser field. The distinct peak structures at the energy shifts of n -photons ($n = +1, +2, +3, +4, +5$, and $+6$) were identified in the observed energy spectrum, and the energy and angular distributions of the LAES signals were in good agreement with those obtained by numerical simulations based on the Kroll-Watson theory. The LAES signal intensities at the scattering angles at 9.1° and 11.8° exhibited a clear plateau structure as a function of the harmonic order n , and the mechanism of these nonperturbative LAES processes was interpreted by a classical mechanical description.

 DOI: [10.1103/PhysRevA.95.023414](https://doi.org/10.1103/PhysRevA.95.023414)

I. INTRODUCTION

Laser-assisted elastic electron scattering (LAES) is a characteristic electron-atom scattering process in a laser field, in which a scattered electron gains or loses its kinetic energy by multiples of the photon energy of the light field, i.e., the kinetic energy gain or loss of the scattered electrons, ΔE , can be expressed as $\Delta E = n\hbar\omega$ ($n = 0, \pm 1, \pm 2, \dots$), where ω is the angular frequency of the light field. This process involves three different kinds of interactions, i.e., the electron-atom interaction, the laser-electron interaction, and the laser-atom interaction, and therefore, the LAES processes afford unique opportunities to investigate the electron dynamics within an atom in an intense laser field [1] as well as to introduce an ultrafast optical gating for probing ultrafast nuclear dynamics within a molecule [2,3].

Kroll and Watson developed a theoretical framework of the LAES processes [4], in which the laser-atom interaction is neglected while the remaining two interactions, i.e., the electron-atom interaction and the laser-electron interaction, are treated in a nonperturbative manner. In this theory, assuming that a laser electric field is written as $\mathbf{F}_0 \sin\omega t$, the differential cross section of the LAES process with the n -photon energy shift, $d\sigma^{(n)}/d\Omega$, is expressed as

$$\frac{d\sigma^{(n)}}{d\Omega} = \frac{|\mathbf{k}_f^{(n)}|}{|\mathbf{k}_i|} J_n^2(\xi) \frac{d\sigma_{el}}{d\Omega}, \quad (1)$$

with

$$\xi = \frac{e}{m_e \omega^2} \mathbf{F}_0 \cdot (\mathbf{k}_i - \mathbf{k}_f^{(n)}), \quad (2)$$

where \mathbf{k}_i and $\mathbf{k}_f^{(n)}$ are electron wave-number vectors before and after the scattering, respectively, $J_n(\xi)$ is the n -th order Bessel function of the first kind, $d\sigma_{el}/d\Omega$ is a differential cross section of the elastic scattering without laser fields; e is the unit charge, and m_e is the mass of the electron.

The LAES process can be categorized into the following three regimes on the basis of the magnitude of the

dimensionless parameter, ξ . When $|\xi| \ll |n|$, the square of the Bessel function in Eq. (1) is approximated as $J_n^2(\xi) \sim |\xi|^{2|n|}/[2^{2|n|}(|n|!)^2]$, and the free-free transition of $\mathbf{k}_f^{(n)} \leftarrow \mathbf{k}_i$ in the LAES process can be treated perturbatively. In this perturbative regime, the LAES signal intensity decreases drastically as the $|n|$ value increases because of $J_{|n|+1}^2(\xi)/J_{|n|}^2(\xi) \sim [\xi/(|n|+1)]^2/4 \ll 1$. On the other hand, when $|\xi| \gg |n|$, the square of the Bessel function in Eq. (1) is expressed as

$$J_n^2(\xi) \sim \frac{1}{\pi|\xi|} [1 - (-1)^n \sin 2|\xi|], \quad (3)$$

and the free-free transition should be treated nonperturbatively. In this nonperturbative regime, the square of the Bessel function oscillates around the central value of $(\pi|\xi|)^{-1}$. Consequently, the intensity of the LAES signals does not vary so much over the wide range of n , and a plateau structure appears in the energy spectrum of the scattered electrons. When $|\xi| \sim |n|$, the LAES processes can be regarded as in the intermediate regime.

The first experimental demonstration of the LAES processes was reported by Andrick and Langhans in 1976 [5]. They observed energy shifts of scattered electrons by $\pm\hbar\omega$ ($n = \pm 1$) through electron scattering by Ar in a laser field whose intensity, I , is $I = 6 \times 10^4 \text{ W/cm}^2$, generated by a continuous-wave midinfrared CO₂ laser with the wavelength (λ) of $\lambda = 10.6 \mu\text{m}$. The $|\xi|$ value was $|\xi| = 0.1$ in their measurement, and therefore, the observed LAES processes are in the perturbative regime. The LAES processes in the nonperturbative regime were reported first by Weingartshofer *et al.* in 1977 [6]. They recorded multiphoton LAES signals up to $n = \pm 3$ in the electron scattering by Ar in a pulsed CO₂ laser field ($\Delta t = 2 \mu\text{s}$, $\lambda = 10.6 \mu\text{m}$, $I \sim 10^9 \text{ W/cm}^2$). The $|\xi|$ value in their measurement was $|\xi| = 15.5$, indicating that the observed LAES processes up to $n = \pm 3$ are all in the nonperturbative regime. Later, Weingartshofer *et al.* [7] performed the LAES measurements with the higher signal-to-noise ratio under the conditions of $|\xi| = 11.5$, and succeeded in recording the multiphoton LAES processes up to $n = \pm 11$, which correspond to the energy shifts up to $\pm 1.29 \text{ eV}$. The plateau structure was identified in the energy spectrum of the LAES signals between $|n| = 1$ and $|n| = 11$.

*Present address: Max-Planck-Institut für Quantenoptik, Hans-Kopfermann-Strasse 1, 85748 Garching, Germany.

†Corresponding author: kaoru@chem.s.u-tokyo.ac.jp

In contrast to the LAES processes in the perturbative regime where LAES processes cannot be treated by classical mechanics, the LAES processes in the nonperturbative regime are considered to be treated classically [4]. In the nonperturbative regime, the motion of an electron in the LAES process can be described by the following three steps: (i) An electron being oscillated by the laser field approaches the target atom, (ii) the electron is scattered by the atom at a certain time, and (iii) the scattered electron escapes from the target atom while it is being oscillated by the laser field. Therefore, when a plateau structure appears in the energy spectrum of the electrons scattered by the LAES processes in the nonperturbative regime, we can discuss differences in the mechanism of the LAES processes of the respective orders, n , in terms of classical trajectories of an electron in the laser field.

In order to discuss the motion of an electron driven by a laser field in the nonperturbative regime ($|\xi| \gg |n|$), the temporal profile of the laser electric field needs to be characterized. Therefore, the LAES measurements performed by single-mode lasers or by mode-locked lasers had been awaited. In 1987, Wallbank and co-workers [8] performed measurements of $n = -1, -2$ LAES processes of Ar with a single-longitudinal-mode CO₂ laser in the nonperturbative regime under the conditions of $|\xi| \leq 6.3$. In 2010, our group [2] recorded the $n = \pm 1$ LAES signals in the electron scattering by Xe in a near-infrared femtosecond intense laser field of a mode-locked Ti:sapphire laser system ($\Delta t = 200$ fs, $\lambda = 795$ nm, $I = 1.8 \times 10^{12}$ W/cm²) under the conditions of $|\xi| \leq 3.9$. We also recorded the LAES signals up to $n = \pm 2$ from CCl₄ and Xe samples under the conditions of $|\xi| \leq 2.4$ [3] and $|\xi| \leq 3.0$ [1], respectively. However, in these studies, the plateau structure, i.e., the direct evidence showing that the LAES processes are in the nonperturbative regime, was not observed, probably because of the limited signal-to-noise ratios, and as a consequence, no attempt has been made to interpret the observed LAES signals classically.

In the present study, in order to observe the plateau structure in the LAES signals induced by the mode-locked laser field, we investigate the LAES processes of Xe in an ultrashort-pulsed near-infrared laser field ($\Delta t = 100$ fs, $\lambda = 800$ nm, $I = 8.8 \times 10^{12}$ W/cm²) using a 1-keV electron beam. The maximum $|\xi|$ under these experimental conditions is estimated to be

$|\xi| = 9.7$, showing that the LAES processes in the range of $|n| \ll 9.7$ are in the nonperturbative regime. From the observation of the high-order multiphoton LAES signals in the range between $n = +1$ and $n = +6$, the clear plateau structures are identified in the LAES signals at the larger scattering angles, and the plateau structures are interpreted well based on the classical mechanical description of the LAES process.

II. EXPERIMENT

Details of the apparatus are described in [3,9]. A pulsed electron beam with the duration of 19 ps accelerated at 1 keV is generated from a home-built photocathode-type electron gun, and the pulsed electron beam collides with a Xe gas beam in a linearly polarized near-infrared ultrashort-pulsed intense laser field ($\lambda = 800$ nm, $\Delta t = 100$ fs, $I = 8.8 \times 10^{12}$ W/cm²). At the scattering point, the electron beam, the atomic beam, and the laser beam cross at right angles with each other, and the polarization direction of the laser field is set to be parallel to the atomic beam axis. The electrons scattered forward in a plane defined by the electron beam axis and the atomic beam axis are introduced into a toroidal-type electron energy analyzer through a thin slit with a 0.8-mm gap, which lies in the plane defined by the electron beam axis and the atomic beam axis. In the electron energy analyzer, the electrons are decelerated to ~ 50 eV, dispersed depending on their energies and scattering angles, and are reaccelerated to their original kinetic energies to hit a two-dimensional position sensitive detector with delay line anodes, so that the energy and angular distributions are recorded as a two-dimensional image without scanning any voltages applied to the analyzer. The scattered electrons with the energy shift range of -1.5 eV $\leq \Delta E \leq +12.0$ eV and the scattering-angle (θ) range of $2.0^\circ \leq \theta \leq 13.4^\circ$ are detected. The electrons in the scattering-angle range of $\theta < 2^\circ$ are blocked by a Faraday cup placed in front of the energy analyzer. The LAES peak profiles appearing in the energy spectrum exhibit a Gaussian distribution whose width is 0.7 eV [full width at half maximum (FWHM)], confirming that the energy resolution is sufficiently high for resolving the neighboring LAES peaks whose energy interval is the one-photon energy of the light field (1.55 eV). A typical count rate of the elastic electron scattering signals is around 300 counts per second, and a total of the accumulation time is 156 h.

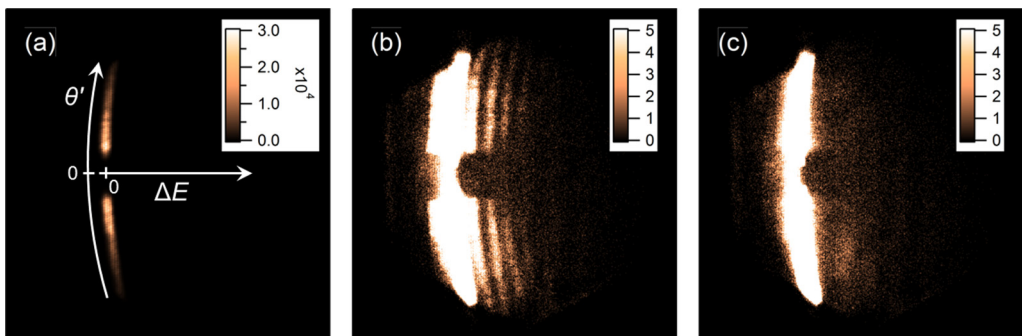


FIG. 1. (a) A raw image of scattered electrons with the laser field. The abscissa for the energy shift, ΔE , is drawn as the straight white arrow and the curved ordinate for the auxiliary scattering angle, θ' , is drawn as the curved white arrow. (b) A rescaled image of (a) for enhancing the visibility of weak signals. (c) A raw image of background signals.

III. RESULTS AND DISCUSSION

Figure 1(a) shows a raw image of the signals of the scattered electrons obtained when the scattering occurred in the laser field, i.e., the electron pulse and the laser pulse arrive at the scattering point simultaneously. In Fig. 1(a), the abscissa represents the energy shift. In the present study, an auxiliary scattering angle (θ') is introduced, which is defined as the electron scattering angle measured from the direction of the incident electron beam on the scattering plane spanned by the incident electron beam axis and the atomic beam axis. When the scattered electron is deflected to the upstream side of the atomic beam, θ' takes a positive value, and, when it is deflected to the downstream side, θ' takes a negative value. Therefore, as represented by the curved ordinate in Fig. 1(a), $\theta' = +\theta$ in the upper half of Fig. 1(a) whereas $\theta' = -\theta$ in the lower half. In Fig. 1(a), the intense elastic scattering signals forming an arcuate line structure can be seen. By rescaling the intensity of the image in Fig. 1(a) so that the visibility of the weak signals is enhanced, Fig. 1(b) was obtained, in which additional weak arcuate line structures appear on the right side of the intense arcuate line of the elastic scattering. In contrast, no such additional arcuate line structures appear in Fig. 1(c), representing the background signals recorded when the timing of the electron beam pulse was delayed by 300 ps with respect to that of the laser pulse so that the scattering occurs in the absence of the laser field. This means that the additional weak arcuate line structures appearing in Fig. 1(b) are the LAES signals. Figure 2(a) shows the energy spectra obtained by integrating the electron signals of Figs. 1(b) and 1(c) along the scattering-angle coordinate over the detectable scattering-angle range. The side-band peaks with the spacing of 1.55 eV are clearly seen in the energy spectrum of electrons scattered in the laser field (red filled circles), while no side-band peaks can be seen in the energy spectrum of the background signals (black open squares). The red filled circles in Fig. 2(b) represent background-subtracted signals obtained by subtracting the background signals with black open squares from the signals with red filled circles in Fig. 2(a), and Fig. 2(c) is an expanded view of the square area enclosed by a broken line in Fig. 2(b). Six distinct peaks with the spacing of 1.55 eV can be recognized in Figs. 2(b) and 2(c).

In order to interpret the recorded LAES spectrum, we performed numerical simulations of the LAES signals based on the Kroll-Watson theory [4], in which the differential cross section of the LAES process with the n -photon energy shift, $d\sigma^{(n)}/d\Omega$, is expressed as Eq. (1). The simulations were performed by taking into account the spatiotemporal overlap among the electron beam, the atomic beam, and the laser beam. In the present simulations, we adopted the literature values of $d\sigma_{el}/d\Omega$ in Ref. [10] as in our previous experimental studies [2,9]. The calculated spectra obtained using the Kroll-Watson formula are shown in Figs. 2(b) and 2(c) with green solid curves. The intensity is scaled so that the intensity of the $n = 0$ LAES signal obtained from the calculation becomes equal to that of the experiment.

The calculated energy spectrum is in good agreement with the experimental energy spectra, showing that the relative intensities of the recorded multiphoton LAES signals in the

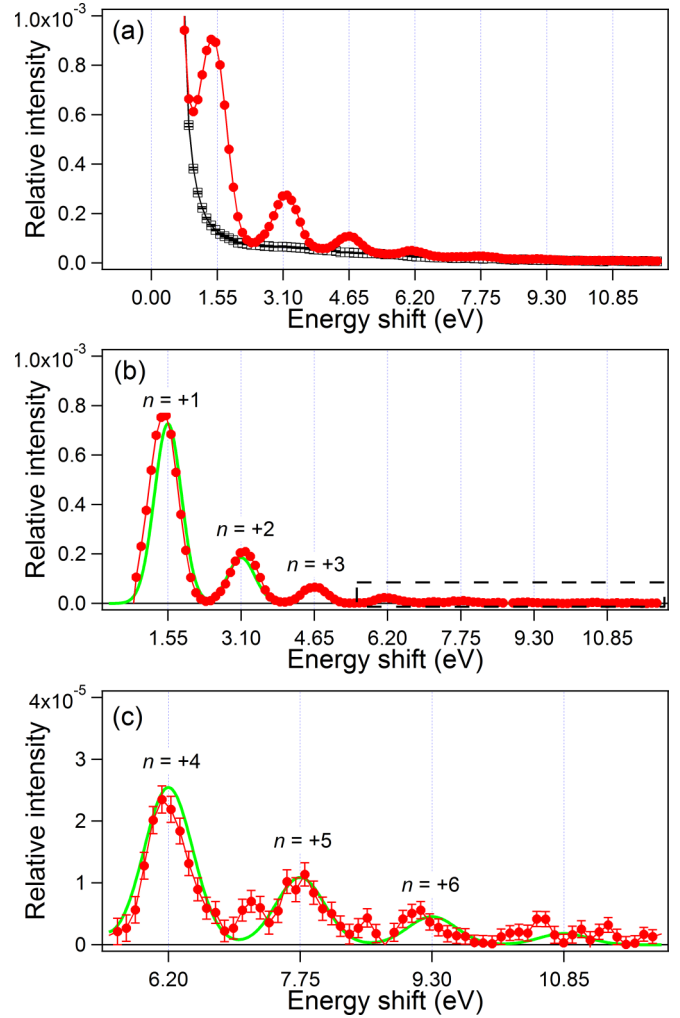


FIG. 2. Energy spectra of relative intensities of scattered electron signals. The relative intensity of each spectrum is normalized by the peak intensity of the elastic scattering signal. Error bars are estimated from the square roots of signal counts. (a) Red filled circles: electron signals with the laser field. Black open squares: background signals. (b) Red filled circles: the background-subtracted signals obtained by subtracting the background signals from the signals with the laser field. Green line: a LAES spectrum calculated by the Kroll and Watson formula [Eq. (1)]. (c) An expanded view of the square area enclosed by a broken line in (b).

range between $n = +1$ and $n = +6$ are well described by the Kroll-Watson theory. It is noteworthy that the observed LAES signals of $n = +6$ correspond to the energy shift of 9.3 eV, which is the largest energy gain ever observed in the LAES experiments. It can be seen in Fig. 2(c) that a small peak appears between the $n = +4$ and $n = +5$ LAES signals and another small peak appears between the $n = +5$ and $n = +6$ LAES signals, which do not appear in the simulated energy spectrum. At the present stage, no interpretations have been made on the origin of these small peaks.

The angular distributions of the electron signals forming the six LAES peak profiles for $n = +1$ to $n = +6$ are shown in Figs. 3(a)–3(f) with red filled circles as a function of θ . The angular distributions of the respective n -photon LAES signals

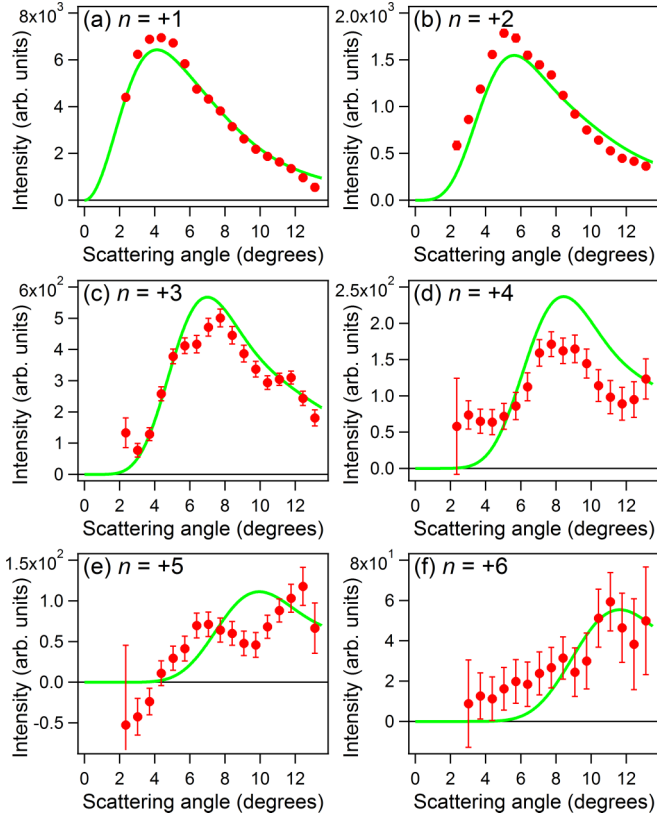


FIG. 3. Angular distributions of the LAES signals of (a) $n = +1$, (b) $n = +2$, (c) $n = +3$, (d) $n = +4$, (e) $n = +5$, and (f) $n = +6$ transitions. Red filled circles: recorded LAES signals. Green solid lines: calculated angular distributions by Kroll-Watson theory. The electrons in the range of $\theta < 2^\circ$ are blocked by a Faraday cup placed in front of the energy analyzer and are not observed.

are obtained by integrating the signals along the energy axis over the energy range of ± 0.58 eV covering the respective LAES peak profile having the FWHM width of 0.7 eV. The peak position in the angular distribution tends to shift towards the larger scattering-angle range as the n increases. Green solid lines in Figs. 3(a)–3(f) show the results of the numerical simulation based on the Kroll-Watson theory. Relatively large discrepancies between the experimental results and the simulated results can be seen in the peak profiles for $n = +4, +5$, and $+6$ shown in Figs. 3(d)–3(f). It is true that the error bars in Figs. 3(d)–3(f) are much larger than those Figs. 3(a)–3(c) for the peak profiles for $n = +1, +2$, and $+3$, reflecting the fact that the signal intensity becomes smaller as n increases, but the general tendencies of the angular distributions are well reproduced by the simulated results in Figs. 3(a)–3(f).

As described in the Introduction, the LAES processes can be categorized into the three regimes in terms of the index value of $|\xi|$ defined in Eq. (2). In the classical mechanical description of the LAES processes in the nonperturbative region [4], an energy shift in the LAES processes induced by a laser electric field of $\mathbf{F}_0 \sin \omega t$ is expressed by

$$\frac{\Delta E}{\hbar \omega} = \xi \cos \omega t_1 = \frac{e \mathbf{A}(t_1) \cdot (\mathbf{k}_i - \mathbf{k}_f)}{m_e \omega}, \quad (4)$$

where t_1 is the time when the electron-atom collision occurs, $\mathbf{A}(t)$ is the vector potential of the laser field, and \mathbf{F}_0 is defined to be directed to the upstream side of the atomic beam. Equation (4) shows that the vector potential at the collision time, $\mathbf{A}(t_1)$, can be determined from the energy shift and the scattering angle of the scattered electron. Consequently, the collision time, t_1 , can be obtained from the relationship of $t_1 = \pm \omega^{-1} \arccos\{\omega[\mathbf{A}(t_1) \cdot \mathbf{F}_0]/|\mathbf{F}_0|^2\} + mT$, where m is an arbitrary integer and T is the period of the laser field. Because $|\cos \omega t_1| \leq 1$, a classical cutoff (ΔE_c) in the energy shift becomes $\Delta E_c = |\xi| \hbar \omega$. It should be noted that the LAES processes with $|\Delta E| > \Delta E_c$ are forbidden in classical mechanics.

Because ξ varies depending on the scattering angle θ as expressed in Eq. (2), the classical cutoff ΔE_c also varies depending on θ . When $|\xi|$ is much higher than $|n|$ at a certain scattering angle, a plateau structure with a cutoff energy of $|\xi| \hbar \omega$ will show up in the energy spectra of the LAES signals. For example, $|\xi|$ values for the equally spaced scattering angles over the detectable angle, i.e., $\theta = 3.7^\circ, 6.4^\circ, 9.1^\circ$, and 11.8° , are $|\xi| = 2.7, 4.7, 6.6$, and 8.6 , respectively, using the absolute value of \mathbf{F}_0 , $|\mathbf{F}_0| = 8.1 \times 10^7$ V/cm, converted from the experimental peak field intensity of $I = 8.8 \times 10^{12}$ W/cm². Therefore, plateau structures are expected to be observed more clearly in the energy spectra at the larger scattering angles.

Figures 4(a)–4(d) are logarithmic plots of the LAES signal intensities as a function of n for the scattering angles of $\theta = 3.7^\circ, 6.4^\circ, 9.1^\circ$, and 11.8° . The red filled circles in Figs. 4(a)–4(d) are the experimental data. In Figs. 4(a)–4(d), the vertical broken lines represent the position of the corresponding cutoff orders, $|\xi|$, and the green solid curves are drawn by connecting the signal intensities simulated by the Kroll-Watson theory for the respective n values. As shown in Figs. 4(c) and 4(d), plateau structures can be identified, showing that these signals in the plateau region are originated from the LAES processes in the nonperturbative regime. This means that the origin of the signals shown in Figs. 4(c) and 4(d) can be described by classical mechanics.

For example, the LAES signals with $n = +1, +2, +3, +4, +5$, and $+6$ at $\theta' = \pm 11.8^\circ$ ($\xi = \mp 8.6$) are originated from the scattering events occurring when the vector potentials, $A(t)$, are $A(t_1) = \pm 4.0 \times 10^{-7}$, $\pm 8.1 \times 10^{-7}$, $\pm 1.2 \times 10^{-6}$, $\pm 1.6 \times 10^{-6}$, $\pm 2.0 \times 10^{-6}$, and $\pm 2.4 \times 10^{-6}$ Vm⁻¹s, respectively, where the vector potentials directed to the upstream side of the atomic beam are represented by positive values. If it is assumed that the scattering occurred around the peak field intensity ($I = 8.8 \times 10^{12}$ W/cm²), the collision times for the respective signals are estimated as shown in Table I. In Table I, the collision times are chosen in the range of $-T/2 \leq t_1 \leq T/2$, and thus these collision times have an arbitrariness of $t_1 + mT$, where m is an integer. Similarly, at $\theta' = \pm 9.1^\circ$ ($\xi = \mp 6.6$), the collision times for the transitions of $n = +1, +2, +3, +4, +5$, and $+6$ are estimated as summarized in Table I. Therefore, each one of the electron scattering signals can be assigned to the scattering event occurring at the specific collision time, t_1 , within the period of the laser field, and slight differences in the collision times of the order of 10 as can be discriminated by the measurements of the plateau structures in the angle-resolved energy spectra of the scattered electrons of the LAES processes in the

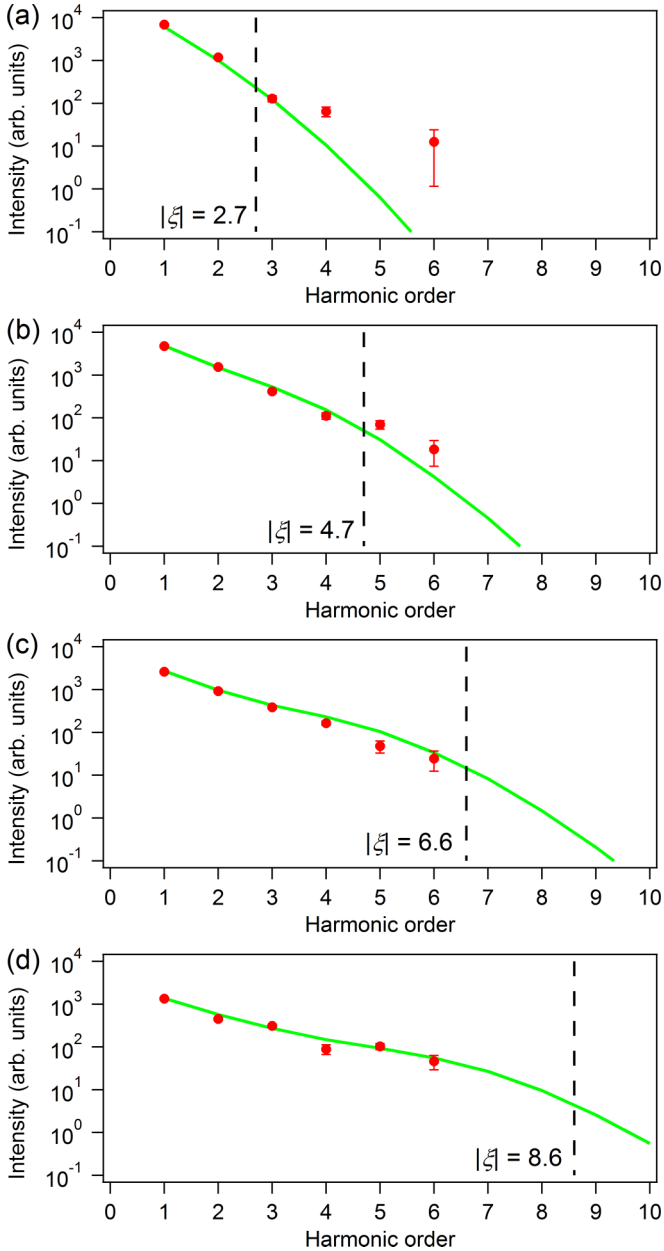


FIG. 4. Logarithmic plots of the LAES signal intensities as a function of n for the scattering angles of (a) $\theta = 3.7^\circ$, (b) $\theta = 6.4^\circ$, (c) $\theta = 9.1^\circ$, and (d) $\theta = 11.8^\circ$. Red filled circles: observed LAES signals. Green solid lines: LAES signals calculated by Kroll-Watson theory. Broken vertical lines represent the positions of the corresponding cutoff orders, $|\xi|$. In (a), the data point at $n = 5$ is absent because the observed signal intensity after the background subtraction at $\theta = 3.7^\circ$ in Fig. 3(e) yielded a negative value.

nonperturbative region. The impact parameter b for the LAES processes at $\theta' = \pm 11.8^\circ$, for example, is estimated to be $b \sim |\mathbf{k}_i - \mathbf{k}_f|^{-1} = 0.30 \text{ \AA}$. Therefore, the length of time required for the interaction between the electron and the atom is estimated to be around 1.6 as, showing that the intrinsic accuracy of t_1 in the present discussion should be around a few attoseconds. This classical mechanical interpretation of the LAES processes in terms of the collision time will be of use for the investigation of ultrafast electron collisions by

TABLE I. The estimated collision times (t_1) for the respective LAES signals.

θ'	ξ	t_1 (fs)					
		$n = +1$	$n = +2$	$n = +3$	$n = +4$	$n = +5$	$n = +6$
+11.8°	-8.6	± 0.72	± 0.77	± 0.82	± 0.87	± 0.93	± 1.00
-11.8°	+8.6	± 0.62	± 0.57	± 0.51	± 0.46	± 0.40	± 0.34
+9.1°	-6.6	± 0.73	± 0.80	± 0.87	± 0.94	± 1.03	± 1.15
-9.1°	+6.6	± 0.60	± 0.54	± 0.47	± 0.39	± 0.30	± 0.18

target atoms and molecules by the measurements of the LAES signals.

IV. CONCLUSION AND FUTURE PROSPECTS

We have observed the multiphoton free-free transitions in the multiphoton LAES processes up to the sixth order by recording the energy distributions and the angular distributions of the scattered electrons through the collision of 1-keV electrons with Xe atoms in the mode-locked femtosecond intense laser field ($\lambda = 800 \text{ nm}$, $\Delta t = 100 \text{ fs}$, $I = 8.8 \times 10^{12} \text{ W/cm}^2$), and have observed the plateau structures of the LAES signals. The observed LAES signals in the plateau structure have been interpreted by the classical mechanical description of LAES processes in terms of the collision time.

There will be two promising future directions in the study of high-order multiphoton LAES processes. One is related to the measurements of the second plateau, and the other is related to the investigation of the light-dressed states of target atoms and molecules:

(i) Several theoretical studies [11–13] predicted that the second plateau-and-cutoff structure will appear in the energy spectra of LAES signals when low-energy incident electrons around several eV are scattered by target atoms in intense laser fields. The mechanism of the appearance of the second plateau structure can be explained by the recollision scenario, i.e., an electron scattered by the electron-atom collision is driven back by the laser field, and is scattered again by the original target atom. Because the recollision event is the second collision process within a fully correlated electron-atom pair created by the first collision process, the observation of the second plateau will afford us a rare opportunity to investigate correlated double collision processes between a single electron and an atom.

(ii) In our recent study of the LAES signal measurements using Xe in the small scattering-angle range [1], the effect of the laser-atom interaction was identified as discrepancies from the Kroll-Watson theory. The discrepancies appearing in the angular distribution of the $n = \pm 1$ LAES signals as a peak profile at small scattering angle ($\theta < 0.5^\circ$) were explained by the effect of the oscillation of the electrons in Xe driven at the laser carrier frequency. The laser-induced dipole model reported by Beilin and Zon [14] and the Born-Floquet theory developed by Faisal [15] predicted that similar effects are expected to appear in the multiphoton LAES signals. According to the theories, the effect of the atomic electrons oscillating at the n -th order harmonic of the laser carrier frequency should appear in the LAES signals with the kinetic

energy shifts of $\pm n\hbar\omega$ in the small scattering-angle region. Therefore, if the measurements of the high-order multiphoton LAES signals are performed in the small scattering-angle region, we will be able to investigate the oscillation of the electron cloud of the target atoms and molecules in an intense laser field with high-frequency fidelity.

ACKNOWLEDGMENTS

This work was supported by JSPS KAKENHI Grant Nos. JP24245003, JP24750011, JP26288004, JP24-4164, and JP15H05696, and by a grant from the Morino Foundation for Molecular Science.

-
- [1] Y. Morimoto, R. Kanya, and K. Yamanouchi, *Phys. Rev. Lett.* **115**, 123201 (2015).
- [2] R. Kanya, Y. Morimoto, and K. Yamanouchi, *Phys. Rev. Lett.* **105**, 123202 (2010).
- [3] Y. Morimoto, R. Kanya, and K. Yamanouchi, *J. Chem. Phys.* **140**, 064201 (2014).
- [4] N. M. Kroll and K. M. Watson, *Phys. Rev. A* **8**, 804 (1973).
- [5] D. Andrick and L. Langhans, *J. Phys. B* **9**, L459 (1976).
- [6] A. Weingartshofer, J. K. Holmes, G. Caudle, E. M. Clarke, and H. Krüger, *Phys. Rev. Lett.* **39**, 269 (1977).
- [7] A. Weingartshofer, J. K. Holmes, J. Sabbagh, and S. L. Chin, *J. Phys. B* **16**, 1805 (1983).
- [8] B. Wallbank, J. K. Holmes, and A. Weingartshofer, *J. Phys. B* **20**, 6121 (1987).
- [9] R. Kanya, Y. Morimoto, and K. Yamanouchi, *Rev. Sci. Instrum.* **82**, 123105 (2011).
- [10] A. Jablonski, F. Salvat, and C. J. Powell, *NIST Electron Elastic-Scattering Cross-Section Database—Version 3.2* (National Institute of Standards and Technology, Gaithersburg, MD, 2010).
- [11] N. L. Manakov, A. F. Starace, A. V. Flegel, and M. V. Frolov, *JETP Lett.* **76**, 258 (2002).
- [12] A. Čerkić and D. B. Milošević, *Phys. Rev. A* **70**, 053402 (2004).
- [13] A. V. Flegel, M. V. Frolov, N. L. Manakov, and A. N. Zheltukhin, *J. Phys. B* **42**, 241002 (2009).
- [14] E. L. Beilin and B. A. Zon, *J. Phys. B* **16**, L159 (1983).
- [15] F. H. M. Faisal, *Theory of Multiphoton Processes* (Plenum, New York, 1987).